Neurotransmitter 2018; 5: e1631. doi: 10.14800/nt.1631; © 2018 by Hugo R. Arias, *et al*.
http://www.smartscitech.com/index.php/nt

RESEARCH ARTICLE

Bupropion inhibits human α3β4 nicotinic acetylcholine receptors by interacting with luminal and non-luminal sites

Hugo R. Arias[1], Dominik Feuerbach[2*], Marcelo Ortells[1*]

[1]*Faculty of Medicine and CONICET, University of Morón, 1708 Morón, Argentina*
[2]*Novartis Institutes for Biomedical Research, Basel, Switzerland*

*These authors contributed equally to this work
Correspondence: Marcelo Ortells
E-mail: mortells@retina.ar
Received: March 04, 2018
Published online: April 09, 2018

In this work, the interaction of (±)-bupropion [(±)-BP] and (±)-2-(*N-tert*-butylamino)-3'-iodo-4'-azidopropiophenone [(±)-SADU-3-72] with the human (h) α3β4 nicotinic acetylcholine receptor (AChR) is determined by functional and structural approaches. The Ca^{2+} influx results indicate that (±)-BP inhibits hα3β4 AChRs with ~2-fold lower potency than that for (±)-SADU-3-72, indicating that this photoreactive analog can be used to further characterize the (±)-BP binding sites. The competition binding results show that (±)-BP binds to the [^{3}H]imipramine sites at desensitized hα3β4 AChRs with ~4-fold higher affinity compared to the resting state. Molecular docking results indicate that both enantiomers of BP and SADU-3-72, in the protonated state, interact with luminal and non-luminal sites. BP interacts with a luminal site which overlaps that for imipramine, and with non-luminal sites located in the transmembrane domain (TMD) at interfacial (+α3/-β4) and α3 intrasubunit sites, and in the TMD-ECD (extracellular domain) junction at the +β4/-α3 and +β4/-β4 interfaces. Our results are consistent with a hα3β4 model where BP and SADU-3-72 bind to overlapping non-luminal sites as well as non-overlapping luminal sites, probably in physiological conditions. This work expands on previous studies supporting the notion that structurally different antidepressants produce their clinical effects by inhibiting distinct AChR subtypes.

Keywords: Nicotinic acetylcholine receptors; Antidepressants; Bupropion; Photoreactive analog; Noncompetitive antagonists; Conformational states

To cite this article: Marcelo Ortells, *et al*. Bupropion inhibits human α3β4 nicotinic acetylcholine receptors by interacting with luminal and non-luminal sites. Neurotransmitter 2018; 5: e1631. doi: 10.14800/nt.1631.

Introduction

The habenulo-interpeduncular pathway has been the focus of interest in the last years because this circuitry directly and indirectly modulates the brain reward system, which is involved in addictive behavior (reviewed in [1]). This cholinergic pathway expresses α3β4* nicotinic acetylcholine receptors (AChRs), which regulate acetylcholine release on interpeduncular neurons [2]. Interestingly, the inhibition of α3β4 AChRs has been considered as the main mechanism underlying the anti-addictive activity of coronaridine congeners [3,4,5]. Additional evidence also supports the view that this AChR subtype mediates nicotine withdrawal symptoms [6] and nicotine-induced antidepressant-like

activity [7]. Importantly, the α3β4 AChR may play an important role in the antidepressant activity elicited by (±)-bupropion [(±)-BP] [8] and N,6-dimethyltricyclo[5.2.1.02,6]decan-2-amine enantiomers [9], as demonstrated by the lack of activity of these drugs on β4-/- mice compared to that on β4+/+ mice.

Previous studies demonstrated that (±)-BP inhibits muscle-type [10-12], α7 [13], hα4β2 [14], and other [15] AChR subtypes by noncompetitive mechanisms [7]. However, a complete characterization of the interaction of (±)-BP with hα3β4 AChRs, key receptors in reward processes, is lacking. In this regard, Ca^{2+} influx, [^{3}H]imipramine binding, and molecular docking and dynamics studies are performed to characterize the functional and structural interaction of (±)-BP with hα3β4 AChRs in different conformational states. Since (±)-SADU-3-72, a photoreactive analog, has been used to characterize the (±)-BP binding sites at *Torpedo* AChRs [12] and also interacts with hα4β2 AChRs [14], the activity of this analog is compared to that for (±)-BP in the hα3β4 AChR. These studies will pave the way for future photolabeling studies at the hα3β4 AChR.

Materials and methods

Materials

[^{3}H]Imipramine (47.5 Ci/mmol) was obtained from PerkinElmer Life Sciences Products, Inc. (Boston, MA, USA) and stored in ethanol at -20°C. Imipramine hydrochloride was purchased from Sigma-Aldrich Chemical Co. (St. Louis, MO, USA). (±)-Epibatidine hydrochloride was obtained from Tocris Bioscience (Ellisville, MO, USA). (±)-Bupropion hydrochloride [(±)-BP] [(±)-2-(*tert*-butylamino)-1-(3-chlorophenyl)propan-1-one] was obtained through the National Institute on Drug Abuse (NIDA) (NIH, Baltimore, MD, USA). (±)-SADU-3-72 was synthesized as described in [16]. Salts were of analytical grade.

Ca^{2+} influx measurements in the HEK293-hα3β4 cell line

The HEK293-hα3β4 cell line was cultured as described previously [3, 4, 17]. Under these conditions, the AChRs are predominantly expressed with the $(\alpha3)_3(\beta4)_2$ stoichiometry [4]. Ca^{2+} influx experiments were performed using the HEK293-hα3β4 cell line using the fluorimetric imaging plate reader (Molecular Devices, Sunnyvale, CA, USA) as previously described [3, 4, 17]. The drugs were preincubated for 5 min, and then (±)-epibatidine (0.1 μM) was added from the agonist plate to the cell plate using the 96-tip pipettor simultaneously to fluorescence recordings for a total length of 3 min.

[^{3}H]Imipramine binding experiments using hα3β4 AChRs in different conformational states

The effect of (±)-BP on [^{3}H]imipramine binding to hα3β4 AChRs in different conformational states was studied as described previously [3, 4, 17]. In this regard, hα3β4 AChR membranes (1.5 mg/mL) were suspended in binding saline buffer (50 mM Tris-HCl, 120 mM NaCl, 5 mM KCl, 2 mM $CaCl_2$, 1 mM $MgCl_2$, pH 7.4) with 15 nM [^{3}H]imipramine in the absence (AChRs are mainly in the resting state) or in the presence of 0.5 μM (±)-epibatidine (desensitized/agonist-bound state), and preincubated for 30 min at RT. Nonspecific binding was determined in the presence of 100 μM imipramine. Radioactivity counting was performed as previously described [3, 4, 17].

The concentration-response data were curve-fitted by nonlinear least squares analysis using the Prism software. The observed IC_{50} values were transformed into inhibition constant (K_i) values using the Cheng-Prusoff relationship [18], using K_d = 0.41 μM, for [^{3}H]imipramine affinity to hα3β4 AChRs [17].

Molecular docking of BP and SADU-3-72 isomers to $h(\alpha3)_3(\beta4)_2$ AChRs

The $h(\alpha3)_3(\beta4)_2$ AChR was built by homology modeling using the X-ray structure (PDB ID: 4PIR; 3.5 Å resolution) of the mouse (m) 5-HT_{3A}R [19] as the template, and employing the programs Modeller 9.8 [20] and SWIFT MODELLER [21]. The homology modeling procedures were described in our previous work [14]. The software used were ClustalW2 [22], for sequence alignment, NAMD [23], for energy minimization, and VEGA ZZ (version 3.0.5.12) as the interface [24]. The Modeller DOPE score [20] was calculated to evaluate the model accuracy compared to that for the original m5-HT_{3A}R X-ray structure. The (R)- and (S)-isomers of BP and SADU-3-72 were modeled in the protonated state and docked in the receptor model using AutoDock Vina as previously described [14].

Molecular dynamics of BP and SADU-3-72 docked to $h(\alpha3)_3(\beta4)_2$ AChR binding sites

The stability of each BP and SADU-3-72 pose within their predicted docking sites was tested performing 20-ns MD simulations using NAMD and CHARMM force field, and VEGA ZZ as interface. The hα3β4 nAChR model was hydrated with a 10 Å minimum thick shell using the program solvate 1.0 [25], which also added the appropriated number of Cl^- and Na^+ to neutralize the system. The model was subsequently minimized using NAMD. The MD protocol includes a timestep size of 1 fs, with 20 timesteps per cycle

Table 1. Inhibitory potency (IC_{50}) of (±)-bupropion and (±)-SADU-3-72 at the hα3β4 AChR determined by Ca^{2+} influx assays

Ligand	IC_{50} (μM) [a]	n_H [b]
(±)-Bupropion	2.3 ± 0.4	1.39 ± 0.11
(±)-SADU-3-72	1.2 ± 0.3	1.11 ± 0.04

[a] The IC_{50} and n_H values were obtained from Figure 2. [b] Hill coefficient.

Table 2. Binding affinity of (±)-bupropion for the [^{3}H]imipramine binding sites at hα3β4 AChRs in different conformational states

Conformational state	K_i [a] (μM)	n_H [b]
Resting/no agonist	98 ± 16	0.93 ± 0.14
Desensitized/agonist-bound	24 ± 4	0.70 ± 0.07

[a] The K_i values were obtained from Figure 3, according to Eq. (1). [b] Hill coefficient.

Table 3. Docking sites of bupropion and SADU-3-72 isomers at the h$(\alpha3)_3(\beta4)_2$ AChR

Domain	Site	Orientation	Isomers	RMSD
Ion Channel	Luminal 1		(S)-BP	3.73 (0.11)
	Luminal 2		(R)-SADU-3-72	3.52 (0.24)
TMD Non-Luminal	Interfacial +α3/-β4		(R)-BP	0.89 (0.01)
			(S)-SADU-3-72	4.45 (0.11)
	Interfacial +β4/-α3		(R)-BP	2.02 (0.12)
ECD-TMD Junction	Interfacial +α3/-β4		(R)-SADU-3-72	4.75 (0.08)
	Interfacial +β4/-α3		(S)-BP	2.66 (0.01)
			(S)-SADU-3-72	3.16 (0.05)
	Intrasubunit α3	Orientation 1	(R)-BP	1.83 (0.07)
		Orientation 2	(R)-SADU-3-72	7.00 (0.63)

Different ligand orientations are defined when more than one overlapping sites are present in the same docking site. The RMSD and its variance values were obtained from the last third steps of the 20 ns MD simulations, according to Eq. (2).

Table 4. Residues involved in the interaction of bupropion and SADU-3-72 isomers to luminal sites at the h$(\alpha3)_3(\beta4)_2$ AChR

Site	Ligand	M2 (position)		
Luminal 1	(S)-BP	α3-S247 (6')	α3-L250, β4-L251 (9')	
		α3-V254, β4-F255 (13')	α3-F255 (14')	
Luminal 2	(R)-SADU-3-72	β4-C239 (-4')	β4-G240 (-3')	*β4-E241 (-2')*
		α3-T243, β4-T244 (2')	β4-I247 (5')	

Residues in bold form H-bonds with the ligand. Residues in *italics* form salt bridges with the ligand.

Table 5. Residues involved in the interaction of bupropion and SADU-3-72 isomers to non-luminal sites located at the TMD interfacial sites of the h$(\alpha3)_3(\beta4)_2$ AChR

Site	Ligand	M1		M2 (position)				M3
+α3/-β4	(S)-BP	β4-P221	β4-L224	α3-L249 (8')	α3-L250 (9')	β4-A252 (10')	α3-T253 (12')	α3-M281
		β4-T225	β4-L228	α3-V254,β4-F255	β4-F256 (14')	α3-L256 (15')	α3-L257 (16')	
				β4-L259 (17')				
	(S)-SADU-3-72	β4-I216	β4-N217	α3-L250 (9')	β4-A252 (10')	β4-L253 (11')	α3-T253 (12')	α3-M281
		β4-I220	β4-C222	α3-V254 (13')	β4-F256 (14')	α3-L256 (15')	α3-L257 (16')	
		β4-L224	β4-L228	α3-T260 (19')				
+β4/-α3	(R)-BP	α3-P220	α3-I224	α3-S247 (6')	α3-L250,β4-L251	α3-S251 (10')	α3-L252 (11')	
			β4-T254 (12')					
			β4-F255 (13')					
			α3-F255 (14')					

Residues in **bold** form H-bonds with the ligand.

(the number of timesteps between atom reassignments). A cutoff value for non-bond energy evaluation of 12 Å was used. A distance of 8 Å for the switching function was used. Pairs of bonded atoms excluded from non-bonded interaction calculations was determined to 1-4, that is, no non-bonded interactions were calculated for lists of 4 consecutive bonded atoms.

The system was heated from 0 to 300 K, increasing the temperature 25 K for every 500 fs (6 ps). Afterwards, a system equilibration was performed during 200 ps followed by the 20-ns production simulation. The temperature of the system was rescaled every 1000 steps to 300K. During the MD simulation, and to reduce computation time, all residues and water molecules outside a 20 Å radius sphere and centered on the corresponding ligand pose were restricted to their original positions whilst those within this sphere were free to move. The same size sphere was used to implement a spherical periodic boundary condition [26].

To estimate the root mean square deviation (RMSD) values with respect to the initial structure the conformations

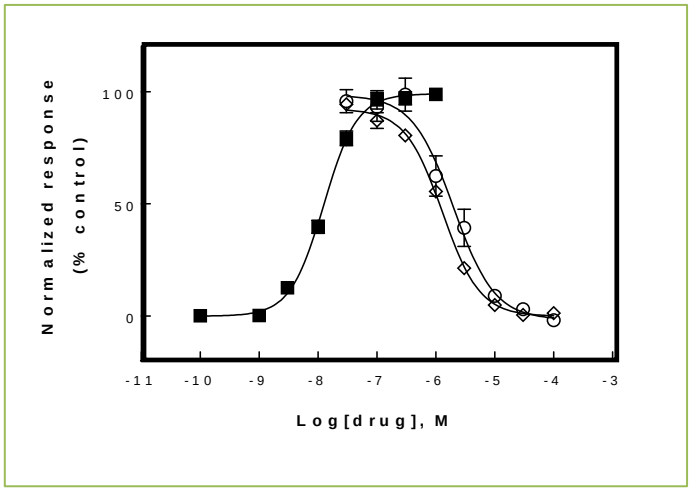

Figure 1. Inhibitory effect of (±)-bupropion and (±)-SADU-3-72 on (±)-epibatidine-induced Ca^{2+} influx in HEK293-hα3β4 cells. Increasing concentrations of (±)-epibatidine (■) activate hα3β4 AChRs with a potency EC_{50} = 13 ± 6 nM (n = 27). Subsequently, cells were pre-treated with several concentrations of (±)-bupropion (○) and (±)-SADU-3-72 (◊), followed by addition of 0.1 μM (±)-epibatidine. Response was normalized to the maximal (±)-epibatidine response which was set as 100%. The plots are the average of seven (○) and six (◊) separate determinations, respectively, where the error bars correspond to the S.D. The calculated IC_{50} and n_H values are summarized in Table 1.

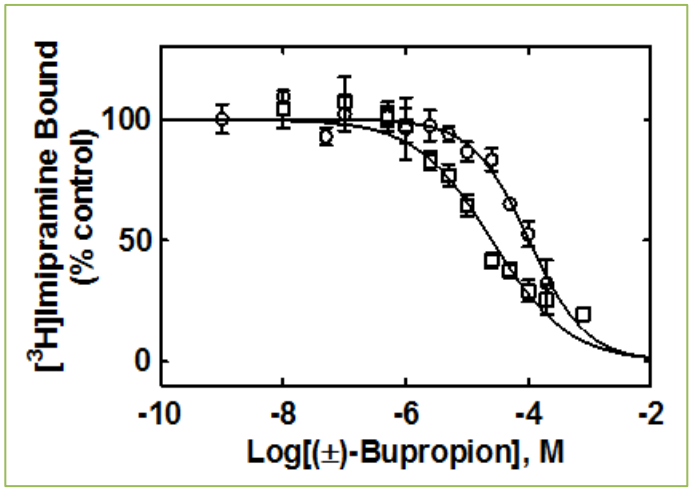

Figure 2. (±)-Bupropion-induced inhibition of [^{3}H]imipramine binding to hα3β4 AChRs in different conformational states. hα3β4 AChR-containing membranes (1.5 mg/mL) were equilibrated (2 h) with 15 nM [^{3}H]imipramine, in the absence (AChRs are mainly in the resting state) (○) or in the presence of 0.5 μM (±)-epibatidine (□) (AChRs are mainly in the desensitized/epibatidine-bound state), and increasing concentrations of (±)-BP. Nonspecific binding was determined at 100 μM imipramine. Each plot is the combination of two separate experiments, where the error bars correspond to the S.D. From these plots the IC_{50} and n_H values were obtained by nonlinear least-squares fit, and the K_i values subsequently calculated using eq 1, and summarized in Table 2.

during the simulation were extracted every 10-ps from the simulation trajectory of 20-ns total time by using VEGA ZZ as previously described [14]. The poses with a RMSD variance value below 1 during the last 5-ns of the MD where considered stable.

To have a theoretical estimation of the ligand binding energies, the Adaptive Poisson-Boltzmann Solver (ABPS) implementation within Vega ZZ [28] was used. Theoretical binding energies were measured from the individual poses between 15 and 20 ns, as previously published [14]. Only the poses with binding energy values ≤ -23 KJ/mol, corresponding to $K_i \leqslant 100$ □M, or binding affinity closer to the experimental value (see Table 2), were used in this work.

Results

Inhibition of (±)-epibatidine-mediated Ca^{2+} influx in hα3β4 AChRs by (±)-BP and (±)-SADU-3-72

(±)-Epibatidine-induced AChR activation was inhibited by pre-incubation with (±)-BP or (±)-SADU-3-72 in a concetration-dependent manner (Fig. 1). The calculated IC_{50} values indicate that (±)-SADU-3-72 is slightly more potent than (±)-BP in inhibiting hα3β4 AChRs (Table 1). The n_H value for (±)-BP is close to unity, whereas the value for (±)-SADU-3-72 is slightly higher than unity (Table 1). These results suggest that the inhibition elicited by these ligands is mainly mediated by a noncooperative mechanism.

(±)-Bupropion-induced inhibition of [^{3}H]imipramine binding to hα3β4 AChRs in different conformational states

The binding affinity of (±)-BP for the [^{3}H]imipramine binding site(s) at the hα3β4 AChR in different conformational states was studied by competition binding experiments (Fig. 2). (±)-BP inhibits [^{3}H]imipramine binding to hα3β4 AChRs in a concentration-dependent fashion, where the affinity for the desensitized sate was ~4-fold higher than that for the resting state (Table 2). The calculated n_H values for (±)-BP are close to unity (Table 2), indicating a noncooperative mechanism.

Molecular docking of BP and SADU-3-72 isomers to the $h(\alpha3)_3(\beta4)_2$ AChR

The final docking site or orientation is the one that the ligand reaches after 15 ns MD simulation. Poses with RMSD variance (VAR) values ≤1 Å, obtained from the MD simulations, and theoretical binding energy (TBE) ≤-23 KJ/mol (corresponding to binding affinities closer to the experimental values; Table 2), were considered stables (Table 3). Molecular docking results showed that protonated BP and SADU-3-72 isomers bind to sites located within the ion channel [i.e., Luminal] and at non-luminal domains, including the transmembrane domain (TMD) and the extracellular-transmembrane (ECD-TMD) junction (Fig. 3;

Table 6. Residues involved in the interaction of bupropion and SADU-3-72 isomers to non-luminal sites located at the ECD-TMD junction of the h(α3)$_3$(β4)$_2$ AChR

Site	Orientation	Ligand	ECD			M1		M2 (position)	M3		M4	
Interfacial +α3/-β4		(R)-SADU-3-72	α3-V46 β4-S46 β4-E49	α3-N47 β4-V47 *β4-E179*	α3-P264 β4-N48 β4-W180		β4-Y214 β4-N217	β4-I263 (21') β4-V264 (22')				
Interfacial +β4/-α3		(R)-BP	β4-L269	*β4-D270*	β4-V271	α3-I215 α3-N216 α3-I219 α3-P220		β4-T254 (12') α3-F255 (14') β4-L257 (15') β4-L258 (16') β4-I260 (18') β4-S261 (19')	β4-G275 β4-L278 β4-M279			
		(S)-SADU-3-72	β4-L269	*β4-D270*	β4-V271	α3-I215 α3-I219 α3-P220 α3-L223 α3-I224	β4-L218	β4-T254 (12') α3-F255 (14') β4-L257 (15') β4-L258 (16') β4-I260 (18') β4-S261 (19')	β4-274 β4-G275 β4-L278 β4-M279			
Intrasubunit α3	1	(R)-BP	P136	F137		T214 I218	L217 C221		I273 L277	Y276 T280	L463 Q466	F464 P467
	2	(R)-SADU-3-72	Y134						L272 Y276	*E275*	Q466	

Residues in **bold** form H-bonds with the ligand. Residues in *italics* form salt bridges with the ligand.

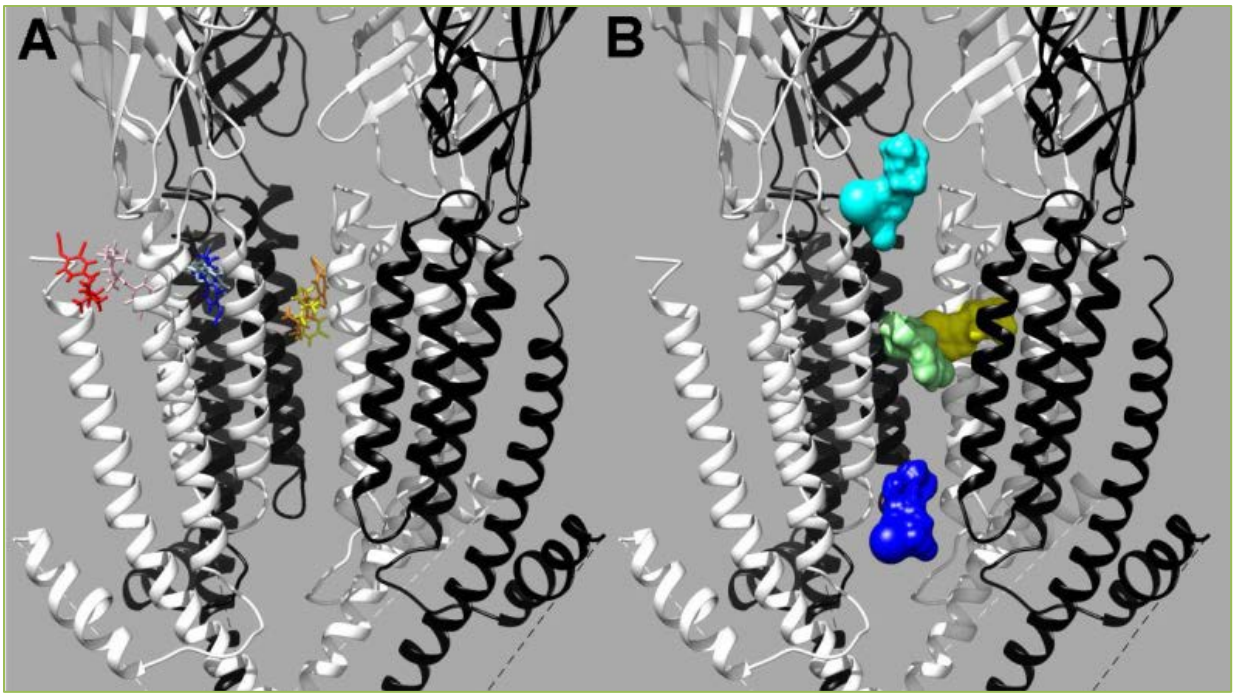

Figure 3. Overlapping (A) and non-overlapping (B) sites for BP and SADU-3-72 isomers at the h(α3)$_3$(β4)$_2$ AChR model. (A) Both BP and SADU-3-72 (represented as sticks) interact with non-luminal sites, including those located at the TMD [i.e., interfacial +α3/-β4 site; (S)-BP = yellow, (S)-SADU-3-72 = orange], and ECD-TMD junction [i.e., interfacial +β4/-α3; (R)-BP = light blue, (S)-SADU-3-72 = dark blue; intrasubunit α3; (R)-BP = pink, (R)-SADU-3-72 = red]. (B) In addition, BP interacts with the luminal 1 site [(S)-BP = light green] as well as non-luminal sites located at the TMD [i.e., interfacial +β4/-α3 site; (R)-BP = yellow], whereas SADU-3-72 interacts with the luminal 2 site [(S)-SADU-3-72 = dark blue] as well as a non-luminal site located at the ECD-TMD junction [i.e., interfacial +α3/-β4, [(S)-SADU-3-72 = cyan]. α3 (white) and β4 (black) subunits are depicted as ribbons. For clarity, an α3 subunit was omitted.

Table 3). Each site could be further discriminated into partially overlapping "orientations", arriving to a total of 10 different docking sites (Table 3).

In general the binding features between BP and SADU-3-72 are quite similar, but differences can also be observed. BP and SADU-3-72 bind to the same receptor sites in three out of the seven found (Fig. 3A). More specifically,

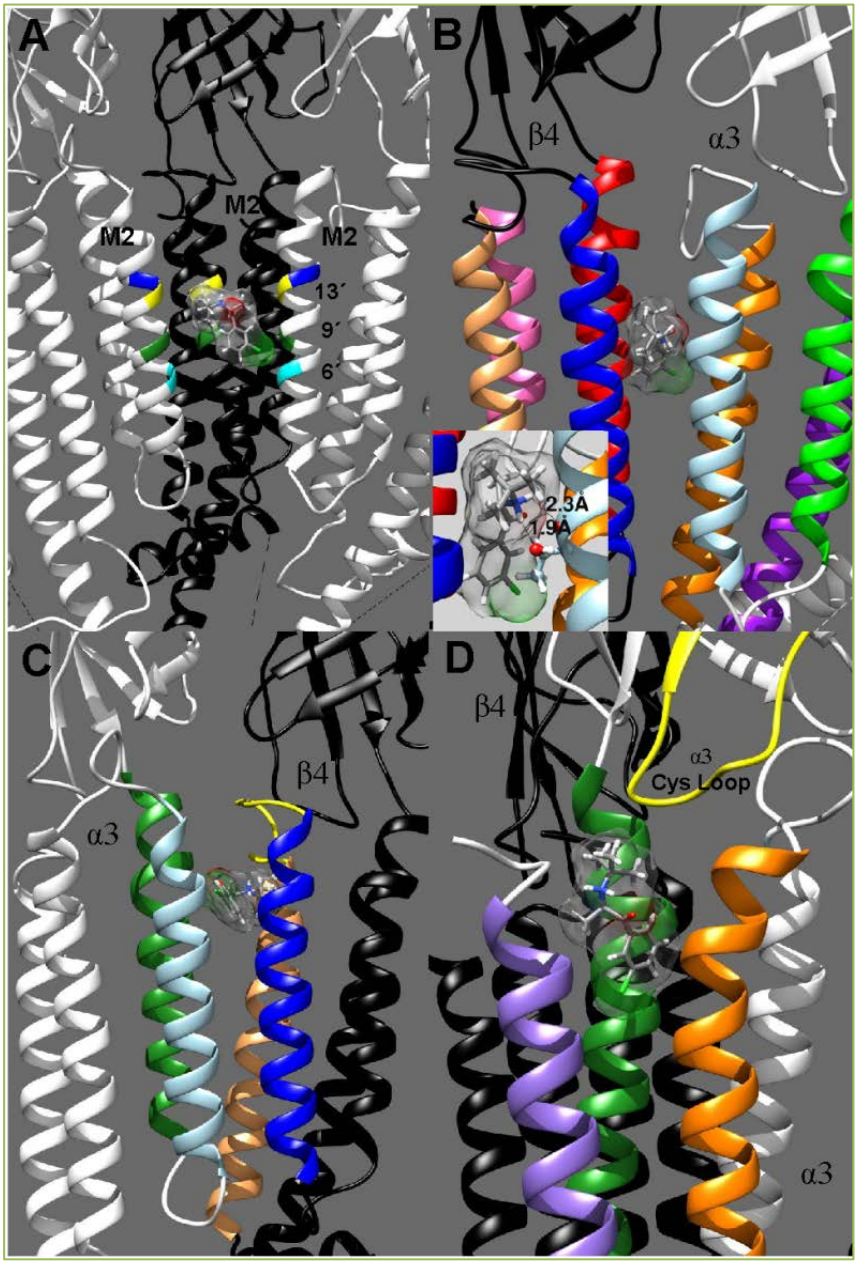

Figure 4. Docking sites for bupropion at the h(α3)$_3$(β4)$_2$ AChR model. (A) Luminal sites for (S)-BP. (S)-BP is depicted as sticks, surrounded by its molecular surface and colored by element: C, grey, N, blue, H, white, O, red, Cl, green. α3 subunits are colored in white and β4 subunits in black, unless otherwise stated. (S)-BP binds to the luminal site formed by the following M2 residues: α3-F255 (14´; blue), α3-V254 and β4-F255 (13´ or valine/phenylalanine ring; yellow), α3-L250 and β4-L251 (9´ or leucine ring; green), and α3-S247 (6´ or serine ring; cyan). (B) Non-luminal TMD site for (S)-BP. α3 subunit: M1 (green), M2 (light blue), M3 (orange), and M4 (purple); β4 subunit: M1 (red), M2 (blue), M3 (light brown), M4 (pink). The inset shows two H-bonds formed between the charged amino group of (S)-BP and the backbone and side chain hydroxyl oxygens from T253, respectively. (C) ECD-TMD junction site for (R)-BP. (R)-BP binds to the interfacial +β4/-α3 site. The ECD residues belong only to the β4-M2-M3 loop (yellow), whereas the TMD residues are from α3-M1 (green), α3-M2 (light blue), β4-M2 (blue), and β4-M3 (light brown). (D) (R)-BP binds to the α3 intrasubunit site (orientation 1), by interacting with Cys-loop (yellow), M1 (green), M3 (orange), and M4 (purple).

both ligands bind to the TMD non-luminal (i.e., interfacial +α3/-β4) and ECD-TMD junctional (i.e., interfacial +β4/-α3 site and α3 intrasubunit site) domains. From the remaining four sites, two belong to SADU-3-72 and two belong to BP (Fig. 3B). Interestingly, BP and SADU-3-72 bind to non-overlapping sites in the ion channel.

Molecular interactions with the ion channel lumen

BP and SADU-3-72 isomers bind to non-overlapping sites in the hα3β4 AChR ion channel lumen (Fig. 4A; Table 3). (S)-BP interacted with the site Luminal 1, formed by M2 residues located at positions 6' (serine ring), 9' (leucine ring), 13' (phenylalanine/valine ring), and 14' (Table 4). For SADU-3-72, another site, Luminal 2, was found much closer to the cytoplasmic side of the ion channel compared to BP. The ligand interacted with residues from positions -4', -3', -2' (intermediate ring), 2' (threonine ring), and 5'.

Molecular interactions with non-luminal sites within the TMD

Two non-luminal sites for BP and SADU-3-72 isomers were found within the TMD, including the interfacial +α3/-β4 and +β4/-α3 sites (Fig. 4B; Table 3). (S)-BP interacted with the interfacial +α3/-β4 site with 20-fold higher TBA than that for the SADU-3-72 isomer. In the +α3/-β4 site, the ligands interacted with a strip of β4-M1 residues, from I216 to L228 as well as with α3-M2 residues [L250 (9'), T253 (12'), V254 (13'), L256 (15'), and L257 (16')] (Table 5). In addition, (S)-BP interacted with α3-L249

(8'), and (S)-SADU-3-72 with T260 (19'). Interestingly, the backbone and side chain hydroxyl oxygens of T253 form H-bonds with the charged amino group of (S)-BP and (S)-SADU-3-72, respectively. (S)-BP interacted with β4-M2 residues, particularly with A252 (10'), F255 (13'), F256 (14'), and L259 (17'), whereas (S)-SADU-3-72 interacted with A252 (10'), L253 (11'), and F256 (14'). (S)-BP and (S)-SADU-3-72 also interact with α3-M3-M281.

(R)-BP is the only one interacting with the +β4/+α3 site, including residues from M1 (i.e., α3-P220 and α3-I224) and M2 [i.e., α3-S247 (6'), α3-L250 and β4-L251 (9'), α3- S251 (10'), α3-L252 (11'), β4-T254 (12'), β4-F255 (13'), and α3-F255 (14')].

Molecular interactions with the extracellular-transmembrane junction domain

In the ECD-TMD junction, several sites were defined at "interfacial" (i.e., +α3/-β4 and +β4/-α3) and "intrasubunit" (at each α3) locations (Table 3). In the +α3/-β4 site, only the SADU-3-72 isomers were found (Table 6). The ECD portion includes residues from the β1-β2 loop, M2-M3 loop, β1 and β9 strands. Interestingly, β4-E179's carboxylic group oxygens form a salt bridge between the protonated N of the ligand and its negatively charged side chain oxygen. The TMD portion, on the other hand, involved M1 and M2 residues (positions 21´ and 22').

In the +β4/-α3 site, (R)-BP (Fig. 4C) and (S)-SADU-3-72 interacted with similar affinity. The ECD residues belong only to β4-M2-M3 loop, where D270 forms salt bridges with both ligands as well as an H-bond with (S)-SADU-3-72, as that described for β4-E179. In the TMD, (R)-BP was bound to α3-M1, α3-M2, and β4-M2 residues (positions 12´, 15´, 16´, 18´, and 19'). The hydroxyl oxygen of S261 formed H-bonds with the amino N of (R)-BP and (S)-SADU-3-72, respectively. (S)-SADU-3-72 also interacted with α3-M1 residues and with β4-L218. Poses at this site also interacted with residues belonging to β4-M3.

An intrasubunit site was also found for BP and SADU-3-72 (Table 6). The α3 intrasubunit site is formed mainly by TMD, but no M2, residues, as well as few ECD residues (i.e., Cys-loop). Two partially overlapping orientations were found (Fig. 4D), one for (R)-BP and another for (R)-SADU-3-72. In orientation 1, (R)-BP interacted with residues from the Cys-loop, M1, M3, and M4 segments, whereas in orientation 2, (R)-SADU-3-72 interacted with different residues from the Cys-loop, M3, and M4 segments.

Discussion

This work is an attempt to compare the interactions of (±)-BP (±)-SADU-3-72 with hα3β4 AChRs, using functional and structural methods.

The Ca^{2+} influx results indicated that (±)-SADU-3-72 is ~2-fold more potent than (±)-BP in inhibiting hα3β4 AChRs (Table 1). In muscle AChR subtypes, this difference was even more pronounced: ~17- and ~6-fold for the hα1β1γδ and hα1β1γδ AChRs, respectively [11], whereas practically no difference was observed in the hα4β2 AChR [14]. Comparing the IC_{50} values (in μM) for (±)-BP at different human AChR subtypes obtained under the same experimental conditions, the following inhibitory potency sequence is observed: hα3β4 (2.3 ± 0.4) (Table 1) > hα4β2 (17.8 ± 2.2) [14] > hα1β1γδ (23.4 ± 4.5) ~ hα1β1εδ (24.4 ± 3.3) [11] >> hα7 (179 ± 20) [13].

Considering that BP can reach brain concentrations of ~10 μM [29], α3β4 AChRs could be inhibited with higher degree compared to other AChR subtypes. α3β4 AChRs are expressed in several brain regions, with preponderance in the cholinergic habenulo-interpeduncular pathway [2]. The inhibition of hα3β4 AChRs by (±)-BP at clinically relevant concentrations support the view that this receptor subtype could be one of the targets related with its clinical efficacy, including antidepressant and smoking cessation properties [7]. The importance of this AChR subtype for the clinical activity of (±)-BP is also supported by the experimental evidence indicating that the antidepressant activity of this ligand is lost in β4-/- mice compared to that observed in β4+/+ mice [8].

The [^{3}H]imipramine competition binding results indicated that (±)-BP binds to the desensitized hα3β4 AChR with ~4-fold higher affinity than that for the resting state (Table 2). A similar trend (~2-fold) was observed for *Torpedo* [10] but not for hα4β2 [14] AChRs. Interestingly, the calculated K_i value for the resting hα7 AChR (63 ± 10 μM) [13] shows a slightly higher affinity than that for the hα3β4 AChR (98 ± 16 μM). These results indicate that the interaction of (±)-BP with the [^{3}H]imipramine binding sites depends on the AChR subtype and on the AChR conformational state. Comparing the K_i values (in μM) for (±)-BP at different AChR subtypes in the desensitized state obtained under the same experimental conditions, the following receptor selectivity is observed: Tα1β1γδ (11.6 ± 1.3) [10] > hα3β4 (24 ± 4) (Table 2) > hα4β2 (29.3 ± 4.2) [14].

The combined results from the Ca^{2+} influx and [^{3}H]imipramine competition binding experiments suggested that (±)-BP inhibits hα3β4 AChRs by interacting with

luminal site(s) [17]. The molecular docking study supports these results, since a luminal site for BP located in a domain formed between the serine (position 6') and threonine/valine (position 13') rings was found in the hα3β4 AChR, which coincides with that characterized for imipramine enantiomers [17,30] and coronaridine congeners [4]. The docking results also showed that BP and SADU-3-72 may interact with a variety of non-luminal sites, supporting molecular mechanisms other than channel blockade such as increased desensitization, as was demonstrated for muscle-type AChRs [10, 11, 7].

Since previous results indicated that BP and SADU-3-72 inhibit hα4β2 [14] and α7 [13] AChRs by interacting with luminal and non-luminal sites, a direct comparison with the observed interaction at the hα3β4 AChR can be done. Both (R)-BP and (R)-SADU-3-72 bind to the hα4β2 ion channel at a site (i.e., between positions -2´ to 9´) partially overlapping both Luminal 1 and 2 sites found in the hα3β4 AChR, whereas BP isomers bind to two overlapping sites at the hα7 AChR ion channel, one closer to the extracellular side (i.e., between positions 13' and 20') compared to the other located between positions 9' and 14´ [13], which corresponds to Luminal 1. In conclusion, the leucine ring is the only structural feature found in the three different receptor subtypes where BP makes contact with. In addition, (S)-SADU-3-72 binds to the hα4β2 AChR at a site equivalent to Luminal 1 in the hα3β4 AChR (between positions 6´ and 13´), whereas BP and SADU-3-72 isomers bind to a site corresponding to Luminal 2 found only for SADU-3-72 in the hα3β4 AChR. In general, BP has a tendency to dock towards the extracellular segment of the ion channel while SADU-3-72 docks predominantly at the cytoplasmic end.

Both BP and SADU-3-72 isomers bind at the non-luminal TMD of the hα3β4 AChR, specifically to the interfacial +α3/-β4 site, whereas only (S)-SADU-3-72 binds at an equivalent position in the hα4β2. Interestingly, the non-luminal sites for coronaridine congeners do not match, beyond a few coincident residues, any site for BP and SADU-3-72 described in the present work. In addition, the M2 segment of the +α3/-β4 site partially overlaps the mixed luminal/non-luminal site found for N,6-dimethyltricyclo[5.2.1.02,6]decan-2-amine enantiomers [30].

Although both SADU-3-72 isomers bind to the ECD-TMD junction at an equivalent site (i.e., interfacial +α3/-β4 site) found for (R)-BP at the hα4β2 AChR, some differences can be described. For example, this site involves similar α and β residues from the ECD and M1 at both receptors, whereas β4- or α4-M2 residues correspond to the respective hα3β4 and hα4β2 AChRs. The M1 and M2 segments of the +β4/-α3 subsite 1 partially overlap the intersubunit site found for N,6-dimethyltricyclo[5.2.1.02,6]decan-2-amine enantiomers [30]. Although this site does not include an ECD segment, it comprises a β4-M3 residue (I289) close to the +β4/-α3 site described here. On the other hand, the interfacial +β4/-α3 subsite 2 for (R)-SADU-3-72 is similar to that found for the same isomer at the hα4β2 AChR, whereas the interfacial +β/-β subsite 1 for both BP isomers and (R)-SADU-3-72 is equivalent to that found only for (S)-SADU-3-72 at the hα4β2 AChR.

In addition to the importance of the ion channel for the inhibitory activity of both SADU-3-72 and BP, the observed agreement between our molecular docking and previous photolabeling results reinforces the significance of the ECD-TMD junction in the interaction of SADU-3-72 with the hα3β4 AChR. For example, M1-Y213 from the *Torpedo* α1 subunit, was photolabeled by [^{125}I]SADU-3-72 in a (±)-BP-sensitive manner when the receptor was in the desensitized state [12]. Our docking results showed that (R)-SADU-3-72 and (R)-BP make contacts with α3-F212 and β4-F213, respectively, the homologous residues of α1-Y213, at the interfacial +β4/-α3 subsite 2. In a previous work, we showed that α4-F217 and β2-F211 from the hα4β2 AChR, also interact with (R)-SADU-3-72 and (R)-BP, respectively [14].

This study shows the functional and structural interaction of BP with α3β4 AChRs in different conformational states. The results indicating that BP and SADU-3-72 isomers bind to overlapping non-luminal sites at the TMD (i.e., +α3/-β4 site) and ECD-TMD junction (i.e., interfacial +β4/-α3 and +β4/-β4 sites), support the view that both ligands may inhibit α3β4 AChRs by allosteric mechanisms different to open channel blockade as well as that (±)-SADU-3-72 could be an excellent photoreactive probe to characterize non-luminal sites in this receptor subtype.

This work expands on previous studies supporting the notion that structurally different antidepressants produce their clinical effects by inhibiting distinct AChR subtypes.

Acknowledgements

The authors thank the National Institute on Drug Abuse (NIDA) for the gift of bupropion.

Conflicting interests

The authors have declared that no conflict of interests exist.

Author Contributions

M.O. performed the molecular docking and molecular dynamics experiments, analyzed results, and wrote part of the manuscript. D.F. performed the Ca^{2+} influx experiments. H.A. designed the experiments, analyzed data, and wrote the majority of the manuscript.

Abbreviations

AChR: nicotinic acetylcholine receptor; NCA: noncompetitive antagonist; (±)-BP: (±)-bupropion [(±)-2-(*tert*-butylamino)-1-(3-chlorophenyl)propan-1-one]; (±)-SADU-3-72: (±)-2-(*N-tert*-butylamino)-3'-iodo-4'-azidopropiophenone; RT: room temperature; BS: binding saline; K_i: inhibition constant; K_d: dissociation constant; IC_{50}: ligand concentration that inhibits 50% binding or Ca^{2+} influx; n_H: Hill coefficient; RMSD: root mean square deviation; DMEM: Dulbecco's Modified Eagle Medium; FBS: fetal bovine serum.

References

1 Ortells MO, Arias HR. Neuronal networks of nicotine addiction. Int J Biochem Cell Biol 2010 42:1931-1935.

2 Grady SR, Moretti M, Zoli M, Marks MJ, Zanardi A, Pucci L, *et al*. Rodent habenulo-interpeduncular pathway expresses a large variety of uncommon nAChR subtypes, but only the αβ4* and αβ3β4* subtypes mediate acetylcholine release. J Neurosci 2009 29:2272-2282.

3 Arias HR, Rosenberg A, Targowska-Duda KM, Feuerbach D, Yuan XJ, Jozwiak K, *et al*. Interaction of ibogaine with human α3β4-nicotinic acetylcholine receptors in different conformational states. Int J Biochem Cell Biol 2010 42:1525-1535.

4 Arias HR, Targowska-Duda KM, Feuerbach D, Jozwiak K. Coronaridine congeners inhibit human α3β4 nicotinic acetylcholine receptors by interacting with luminal and non-luminal sites. Int J Biochem Cell Biol 2015 65:81-90.

5 Alper KR, Lotsof HS, Kaplan CD. The ibogaine medical subculture. J Ethnopharmacol 2008 115:9-24.

6 Dani JA, De Biasi M. Mesolimbic dopamine and habenulo-interpeduncular pathways in nicotine withdrawal. Cold Spring Harb Perspect Med 2013 3. DOI: 10.1101/cshperspect.a012138

7 Arias HR, Biała G, Słomka MK-, Targowska-duda K, Biala G, Kruk-Slomka M, *et al*. Interaction of nicotinic receptors with bupropion: Structural, functional, and pre-clinical perspectives. Recept Clin Investig 2014 1:30-45.

8 Radhakrishnan R, Santamaría A, Escobar L, Arias HR. The β4 nicotinic receptor subunit modulates the chronic antidepressant effect mediated by bupropion. Neurosci Lett 2013 555:68-72.

9 Targowska-Duda KM, Jozwiak K, Arias HR. Role of the nicotinic receptor β4 subunit in the antidepressant activity of novel N,6-dimethyltricyclo[5.2.1.02,6]decan-2-amine enantiomers. Neurosci Lett 2013 553:186-190.

10 Arias HR, Gumilar F, Rosenberg A, Targowska-Duda KM, Feuerbach D, Jozwiak K, *et al*. Interaction of bupropion with muscle-type nicotinic acetylcholine receptors in different conformational states. Biochemistry 2009 48:4506-4518.

11 Arias HR, Feuerbach D, Targowska-Duda KM, Aggarwal S, Lapinsky DJ, Jozwiak K. Structural and functional interaction of (±)-2-(N-tert-butylamino)- 3′-iodo-4′-azidopropiophenone, a photoreactive bupropion derivative, with nicotinic acetylcholine receptors. Neurochem Int 2012 61:1433-1441.

12 Pandhare A, Hamouda AK, Staggs B, Aggarwal S, Duddempudi PK, Lever JR, *et al*. Bupropion binds to two sites in the Torpedo nicotinic acetylcholine receptor transmembrane domain: A photoaffinity labeling study with the bupropion analogue [125I]-SADU-3-72. Biochemistry 2012 51:2425-2435.

13 Vázquez-Gómez E, Arias HR, Feuerbach D, Miranda-Morales M, Mihailescu S, Targowska-Duda KM, *et al*. Bupropion-induced inhibition of α7 nicotinic acetylcholine receptors expressed in heterologous cells and neurons from dorsal raphe nucleus and hippocampus. Eur J Pharmacol 2014 740:103-111.

14 Arias HR, Feuerbach D, Ortells MO. Bupropion and its photoreactive analog (±)-SADU-3-72 interact with luminal and non-luminal sites at human α4β2 nicotinic acetylcholine receptors. Neurochem Int 2016 100:67-77.

15 García-Colunga J, Godoy-García U, Vázquez-Gómez E. Interaction of bupropion and zinc with neuronal nicotinic acetylcholine receptors. Neuropharmacology 2011 61:1202-1209.

16 Lapinsky DJ, Aggarwal S, Nolan TL, Surratt CK, Lever JR, Acharya R, *et al*. (±)-2-(N-tert-Butylamino)-3′-[125I]-iodo-4′-azidopropiophenone: A dopamine transporter and nicotinic acetylcholine receptor photoaffinity ligand based on bupropion (Wellbutrin, Zyban). Bioorganic Med Chem Lett 2012 22:523-526.

17 Arias HR, Targowska-Duda KM, Feuerbach D, Sullivan CJ, Maciejewski R, Jozwiak K. Different interaction between tricyclic antidepressants and mecamylamine with the human α3β4 nicotinic acetylcholine receptor ion channel. Neurochem Int 2010 56:642-649.

18 Cheng Y, Prusoff WH: Relationship between the inhibition constant (Ki) and the concentration of inhibitor which causes 50 percent inhibition (IC50) of an enzymatic reaction. Biochem Pharmacol 1973 22:3099-3108.

19 Hassaine G, Deluz C, Grasso L, Wyss R, Tol MB, Hovius R, *et al*. X-ray structure of the mouse serotonin 5-HT3 receptor. Nature 2014 512:276-281.

20 Sali A, Blundell TL, Comparative protein modelling by satisfaction of spatial restraints. J Mol Biol 1993 234:779-815.

21 Mathur A, Shankaracharya, Vidyarthi AS. SWIFT MODELLER: A JAVA based GUI for molecular modeling. J Mol Model 2011 17:2601-2607.

22 Thompson JD, Higgins DG, Gibson TJ. CLUSTAL W: Improving the sensitivity of progressive multiple sequence alignment through sequence weighting, position-specific gap penalties and weight matrix choice. Nucleic Acids Res 199422:4673-4680.

23 Phillips JC, Braun R, Wang W, Gumbart J, Tajkhorshid E, Villa E, *et al*. Scalable molecular dynamics with NAMD. J Comput Chem 2005 26:1781-1802.

24 Pedretti A, Villa L, Vistoli G. VEGA - An open platform to develop chemo-bio-informatics applications, using plug-in

architecture and script programming. J Comput Aided Mol Des 2004 18:167-173.

25 Grubmüller H. SOLVATE v. 1.0. Theoretical Biophysics Group, Institute for Medical Optics, Ludwig-Maximilians University, Munich. 1996;

26 Lewars EG. Computational chemistry: Introduction to the theory and applications of molecular and quantum mechanics. 2011. DOI: 10.1007/978-90-481-3862-3

27 Arias HR, Fedorov NB, Benson LC, Lippiello PM, Gatto GJ, Feuerbach D, *et al*. Functional and structural interaction of (-)-reboxetine with the human α4β2 nicotinic acetylcholine receptor. J Pharmacol Exp Ther 2013 344:113-123.

28 Baker NA, Sept D, Joseph S, Holst MJ, McCammon JA. Electrostatics of nanosystems: Application to microtubules and the ribosome. Proc Natl Acad Sci U S A 2001 98:10037-10041.

29 Hsyu P-H, Singh A, Giargiari TD, Dunn JA, Ascher JA, Johnston JA. Pharmacokinetics of bupropion and its metabolites in cigarette smokers versus nonsmokers. J Clin Pharmacol 1997 37:737-743.

30 Arias HR, Targowska-Duda K, Jozwiak K. N,6-dimethyltricyclo[5.2.1.02,6]decan-2-amine enantiomers interact with the human α3β4 nicotinic receptor at luminal and non-luminal binding sites. J Biochem Mol Biol Res 2015 1:19-24.

Supplementary Materials

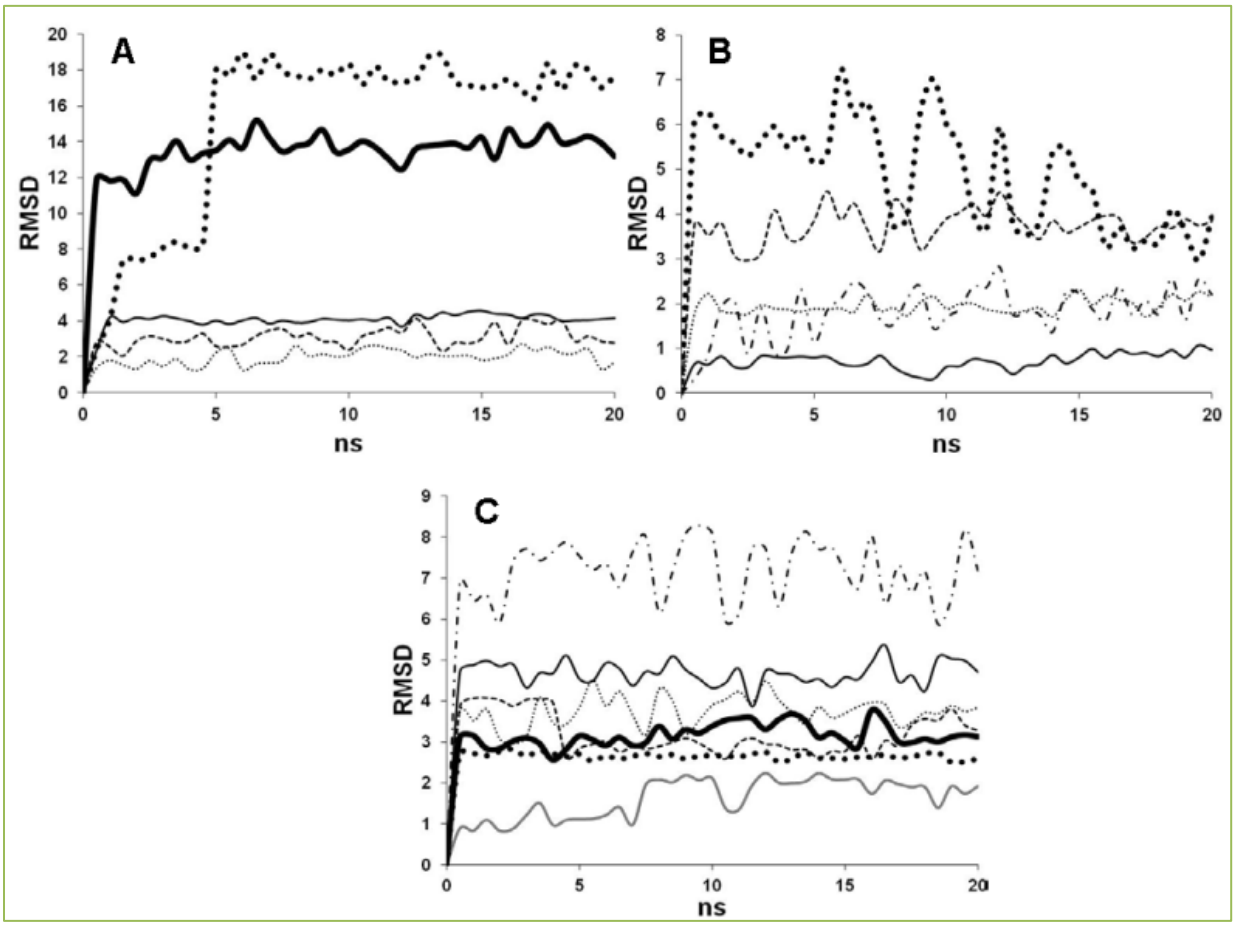

Figure 1S. Molecular dynamics results for BP and SADU-3-72 isomers interacting to luminal (A) and non-luminal sites located at the TMD (B), ECD (C), and ECD-TMD junction (D) of the $h(\alpha3)_3(\beta4)_2$ AChR. RMSD plots for the interaction of: (A) (R)-BP (·····) and (S)-BP (——) with luminal 1 site, and (R)-SADU-3-72 [orientation 1 (- - - -) and orientation 2 (▪▪▪▪▪)] and (S)-SADU-3-72 [orientation 2 (▬▬)] with luminal 2 site; (B) (S)-BP (·····), (R)-BP (——), (S)-SADU-3-72 (- - - -), and (R)-SADU-3-72 (▪▪▪▪▪) with the interfacial +α3/-β4 site; (R)-BP with the interfacial +β4/-α3 (-·-·-·-); (C) (R)-SADU-3-72 (·····) and (S)-SADU-3-72 (——) with the interfacial +α3/-β4 site, and of (R)-BP (----), (S)-BP (▪▪▪▪▪), and (S)-SADU-3-72 (▬▬) with the interfacial +β4/-α3 subsite 1; (R)-BP [orientation 1 (═══)] and (R)-SADU-3-72 [orientation 2 (-··-··-)] with the intrasubunit α3 site. The RMSD, and its variance, values are summarized in Table 3.